Progress In Electromagnetics Research C, Vol. 90, 253–263, 2019

Unsymmetrical Finger-Shape DGSs for Developing a Compact, High-Order, Harmonic-Suppressed Bandpass Filter

Yih-Dar Chen and Chien-Hao Liu*

Abstract—Defected ground structures (DGSs) are often utilized in planar filters and antennas for compactness and spurious frequency suppressions by creating defects or slots on the ground planes. One disadvantage of conventional DGS filters is that the overall dimension increases as the order of the filter increases. In this research, we proposed an asymmetric finger-shape DGS which created multiple equivalent LC resonators when combining with a capacitive microstrip gap on the top. In contrast to the conventional high-order DGS filter by generating many DGSs on the ground plane, the finger-shape DGS provided a high-order bandpass response with one single DGS due to the capacitances between the top metallic strip and the ground plane. Therefore, we developed a wide-band, high-order, and spurious frequency suppressed microstrip bandpass filter with a compact size. To achieve these features, different filter design techniques were exploited including stepped impedance resonator (SIR), series-coupled resonator, and finger-shape DGSs. The main advantage of our DGS filter was that it had a higher-order and wider bandpass responses than other harmonic-suppressed work. A prototype was designed, fabricated, and measured with a calibrated vector network analyzer (VNA) where the simulations matched with the measurements. The finger-shape DGS filter demonstrated a passband centered at 2.35 GHz with a fractional bandwidth of 72.3%, the spurious frequency suppression up to $8.5f_0$ where f_0 was the center frequency of the passband, and a compact size of $0.034\lambda_0^2$ where λ_0 was the wavelength corresponding to f_0.

1. INTRODUCTION

Planar microstrip filters have been widely used in microwave and mm-wave applications for providing band-pass, band-stop, low-pass, and high-pass responses. They can be easily fabricated and integrated with IC and planar antennas such as RFIC and monolithic microwave integrated circuit (MMIC). Recently, with the fast developments of 4G LTE and 5G, the demands of sharp roll-off responses and compact sizes for microstrip filters increase rapidly. For instance, a 4G LTE duplexer needs steep band-edge filtering responses for the transmit and receive bandpass filters to eliminate signal interferences and leakages. Two general approaches of obtaining steep skirt selectivity are increasing the order of the filter or utilizing high-Q mechanical devices such as acoustic wave (SAW) filters and bulk acoustic wave (BAW)-based filters [1]. For planar filters, the high-order responses are implemented by creating multiple equivalent LC resonators coupled together using microstrip lines or coupled lines. The drawback of high-order filters is that the occupied area increases as the order increases. For high-order responses and compact sizes, defected ground structures (DGSs) are often exploited in microstrip filters by creating defects or slots on the ground plane. A DGS is essentially a resonance due to the inductive current path along the slot and the capacitive gap within the slot. For example, the commonly-seen dumbbell-shape DGS implemented with microstrip lines is modeled as an equivalent parallel resonator with a first-order

Received 17 November 2018, Accepted 2 February 2019, Scheduled 5 March 2019
* Corresponding author: Chien-Hao Liu (cliu82@ntu.edu.tw).
The authors are with the Department of Mechanical Engineering, National Taiwan University, Taipei 10617, Taiwan.

bandstop response. By creating multiple resonators on the top microstrip and bottom ground plane, the overall size of a DGS microstrip filter is smaller than a regular microstrip filter with the same order.

In addition to the order and geometric size, one important parameter needs to be considered for planar microstrip filters is the undesired harmonics (i.e., spurious frequency) occurring in the high frequency bands. Spurious frequencies can lead to unwanted out-of-band emissions or deteriorations of communication systems. Various spurious-frequency suppressed bandpass filters have been investigated by different groups [2–6]. Most of them utilize stepped impedance resonators(SIRs) with the high-stopband-rejection characteristics to suppress spurious frequencies. Some examples of SIR-based bandpass filters demonstrate narrow passband bandwidths and harmonics suppressions [7, 8]. For wide-band applications, the passband bandwidth of SIR filter can be enlarged by increasing the order of the filter or the inductance values of parallel resonators. As mentioned before, increasing the order of the filter can result in a wide bandwidth and a sharp roll-off response but it also increases the overall size by adding more resonators. For planar microstrip filter design, there is a trade-off between the order, bandwidth, and overall size.

In this research, we proposed a compact, high-order, harmonic-suppressed bandpass microstrip filter by combining the aforementioned techniques including SIRs, series-coupled resonator, and finger-shape DGSs. The purpose of this work was to create multiple equivalent LC resonators at the region of the finger-shape DGS for miniaturization. In addition, the strong inductance of the finger-shape DGS contributed to spurious frequency suppressions as well. By combining the SIR and finger-shape DGS, the microstrip filter had a high-order bandpass response and harmonics suppressions within a compact size.

This paper was organized as follows. In the next section, the principles of filter design techniques were described. The design procedures of the proposed filter was presented and verified with full-wave EM simulations. Then, a prototype was fabricated with standard PCB photolithography and measured with a calibrated vector network analyzer (VNA). Finally, we discussed the filter characteristics and concluded with a summary of our results.

2. THEORY AND DESIGN PROCEDURES

The goal of this research was to design a bandpass filter with a passband covering the ISM band with wide bandwidth and a sharp roll-off response with a large out-of-band rejection up to 20 GHz. Fig. 1 shows the 3D topology of the proposed finger-shaped DGS bandpass filter composed of two 50 Ohms transmission feed lines, a series-coupled SIR, and two finger-shape DGSs on the ground plane. Each DGS was composed of a hollow rectangular defect containing a finger-like structure in order to increase the current path of the DGS for creating large inductance. The geometric dimensions of the device were listed in Table 1.

The first step was to design the series-coupled SIR that its resonant frequency operated at the

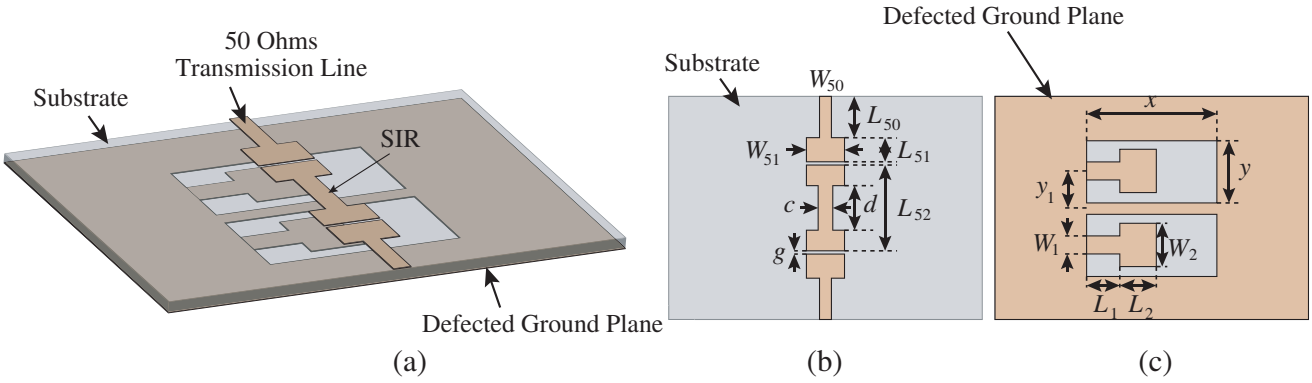

Figure 1. (a) The 3D topology of the proposed finger-shape DGS bandpass filter. (b) The top view. (c) The bottom view. The geometric dimensions were listed in Table 1.

Table 1. Geometric dimensions of the finger-shape DGS bandpass filter shown in Fig. 1.

Para.	Value (mm)	Para.	Value (mm)	Para.	Value (mm)
W_{50}	1.01	W_{51}	6.2	L_{50}	7.6
L_{51}	7	L_{52}	14.3	c	1
d	3	g	0.2	x	16.8
y	10.5	y_1	7.4	W_1	2
W_2	5.5	L_1	7	L_2	5.5

ISM band. Since a single SIR had a narrow bandwidth and the unwanted harmonics were still in the frequency range that we were interested. Then, the aforementioned finger-shape DGS was utilized to increase the bandwidth and reduce the harmonics. The detailed design procedures were described as follows.

2.1. Design of SIR

Stepped impedance resonator (SIR) is often exploited in bandpass filters for harmonics or spurious frequency suppressed applications. SIR is essentially a non-uniform microstrip lines composed of high and low impedances where the spurious frequencies can be altered by changing the impedance ratio and the corresponding electrical lengthes [7–9]. Fig. 2 shows two cases of SIR composed of two different microstrip lines with impedance of Z_1 and Z_2 and the corresponding electrical lengthes of θ_1 and θ_2. The impedance ratio, K, is define as Z_2/Z_1 where $0 < K < 1$ corresponds to the case when the impedance at center is larger than the impedances at both sides shown in Fig. 2(a) and vise versa shown in Fig. 2(b). In general, the SIR have different electrical lengths for high and low impedances (i.e., $\theta_1 \neq \theta_2$). Based on the fundamental resonant condition, the total electrical length of the SIR can be expressed in terms of the electrical length of θ_1 and the impedance ratio:

$$\theta_T = \begin{cases} 2\tan^{-1}\left(\dfrac{1}{1-K}\left(\dfrac{K}{\tan\theta_1}+\tan\theta_1\right)\right) & \text{if } K \neq 1 \\ \pi & \text{if K=1} \end{cases} \tag{1}$$

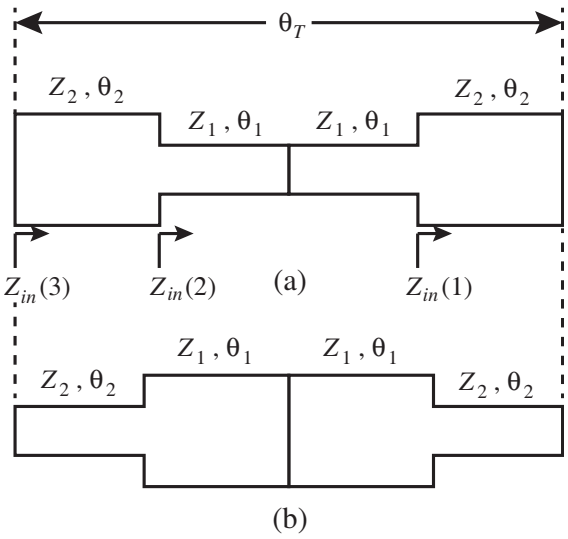

Figure 2. The schematic diagram of two microstrip SIRs. (a) The impedance ratio $0 < K < 1$. (b) The impedance ratio $K > 1$.

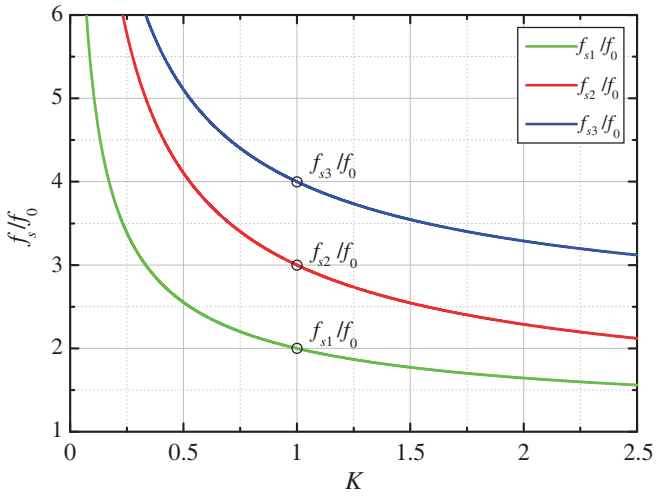

Figure 3. For $(\theta_1 = \theta_2)$, the spurious frequencies are functions of the impedance ratio. For $K = 1$, the first spurious frequency is twice as many as the fundamental resonant frequency. For $K < 1$, the first spurious frequency can be two times larger than the fundamental resonant frequency. Similarly, other spurious frequencies are much larger than the fundamental resonant frequency. In other words, the undesired harmonic frequencies of SIRs can be shifted to a high frequency band for for $K < 1$.

The total electrical length of the SIR has a minimum value when $0 < K < 1$ and the condition can be obtained by differentiating Eq. (1) with respect to θ_1:

$$\frac{1}{1-K}\left(\tan^2\theta_1 - K\right)\sin^2\theta_1 = 0 \tag{2}$$

In Fig. 3, it is demonstrated that when $K = 1$, the first spurious frequency, f_{s1}, is twice as much as the fundamental resonant frequency, f_0, as observed in a general half-wavelength resonator. The second and third spurious frequencies are three and four times as many as the fundamental resonant frequency. However, when $0 < K < 1$, the first spurious frequency is two times larger than the fundamental frequency. Similarly, other spurious frequencies are much larger than the fundamental frequency. In other words, the undesired harmonic frequencies of SIRs can be shifted to a higher frequency band when

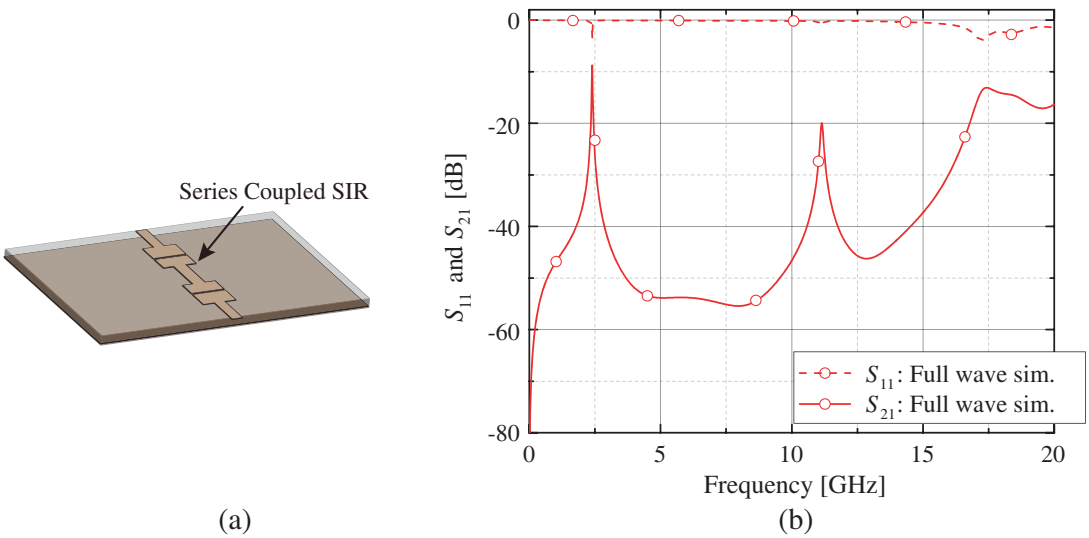

Figure 4. (a) 3D topology of a series-coupled SIR. (b) Simulated transmission and reflection coefficients obtained from full-wave EM simulations. The fundamental resonant frequency was at 2.4 GHz and harmonic frequencies were observed in the frequency range from 0 to 20 GHz.

the impedance ratio is smaller than 1. However, the spurious frequencies of SIRs can be shifted closer to the fundamental frequency for $K > 1$.

For designing a harmonic-suppressed SIR microstrip bandpass filter, the impedance ratio, K, should be much smaller than 1 for short electrical length and shifting spurious frequencies to a higher frequency band. K was chosen to be 0.15 based on Eq. (1) and Eq. (2) for obtaining the minimum total electric length of 72.7°. The SIR microstrip filter was designed to have a fundamental resonant frequency of 2.4 GHz shown in Fig. 4(a). The geometrical length of the SIR filter was 15 mm which was shorted than that of a uniform SIR filter of 35.2 mm. The simulated transmission and reflection coefficients obtained from full-wave EM simulations were shown in Fig. 4(b). Although K was as small as possible to shift the spurious frequencies away from the fundamental resonant frequency, harmonics still occurred within the interested frequency range (i.e., 0 to 20 GHz). In addition, the SIR filter needed optimization for reducing the insertion loss due to the under-coupled response and increase the bandwidth by increasing the number of resonators.

2.2. Design of Finger-Shape DGSs

In general, DGSs are implemented via creating defects or slots on the ground plane of transmission lines in order to disturb the current distributions on the ground plane and result in slow-wave effects. Various patterns have been developed for different applications such as U-shape and meander lines. For a commonly-used dumbbell-shape DGS, it is modeled as a parallel LC resonator with a bandstop response. The equivalent inductance and capacitance values can be expressed as:

$$C = \frac{f_c}{4\pi Z_0 \left(f_o^2 - f_c^2\right)} \tag{3}$$

$$L = \frac{1}{(2\pi f_0)^2 C} \tag{4}$$

where f_c is the cutoff frequency, and f_0 is the resonant frequency [10–14]. Similarly, a different pattern of a DGS can produce a resonance on the ground plane resulting in a bandstop response. Therefore, a high-order bandstop response can be obtained by arranging multiple DGSs on the ground with appropriately coupling.

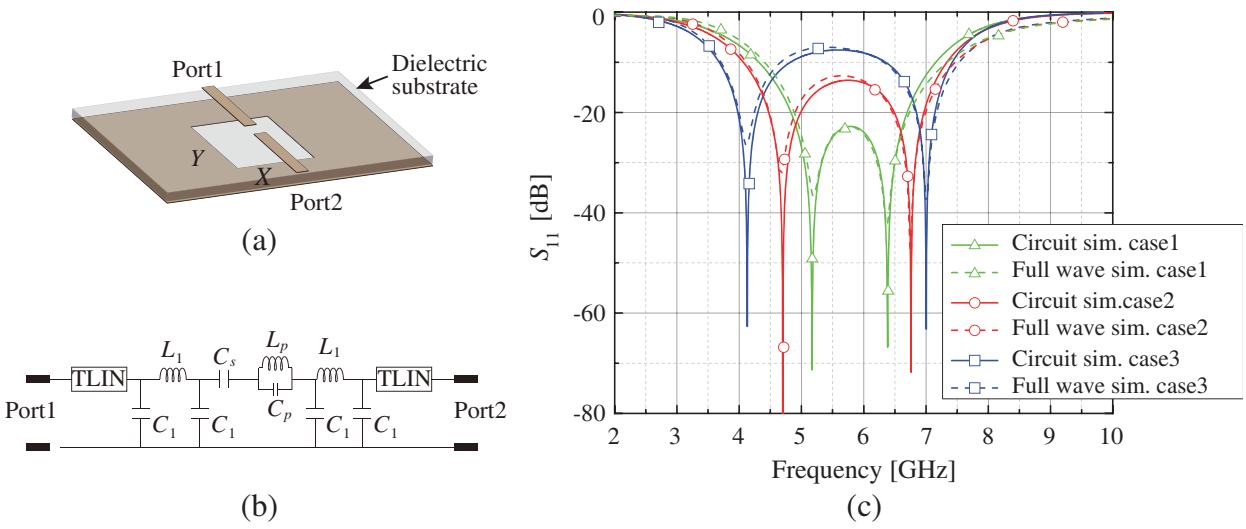

Figure 5. (a) A rectangular-DGS bandpass filter composed of a capacitive gap microstrip and a rectangular defect on the ground plane. (b) The equivalent circuit model. (c) The simulated reflection coefficients obtained from the equivalent circuit model and the full-wave EM simulations. As the width of rectangular DGS increases, the capacitance between top and bottom conductors decreases and affects the transmission band.

For practical applications or complicated geometrises, the capacitances between the top metallic strips and DGSs need to be taken into account. For the DGS microstrip line, the currents focus on the non-intact edge of the ground plane and the E-field densities at both sides are stronger than those at the center. Since the E-field densities are weak at the center due to the opening of the DGS, the capacitances between the top conductor and the ground plane are reduced and some portions of electromagnetic wave energy spread out from the opening resulting in undesired radiations. These capacitance are often considered as parasitic capacitances which cause undesired spurious frequencies. However, the top-bottom capacitances are beneficial for our designs of finger-shape DGSs. In addition to providing bandstop responses, DGSs can be exploited in designing lowpass or bandpass microstrip filters. Fig. 5(a) shows a DGS-based bandpass filter composed of a capacitive gap microstrip line and a rectangular defect on the ground. Fig. 5(b) shows its equivalent circuit model where C_1 indicates the capacitance between the top and bottom conductors, C_s is the capacitance of microstrip gap, and L_1 is the inductances of the microstrip on both sides. A second-order bandpass response is obtained from the inductors of the microstrip, L_1, and the series capacitor, C_s separated by the top-bottom capacitors, C_1 where the bandstop response of the parallel LC resonator due to the rectangular DGS is out of interested frequency band. The width of the rectangular DGS is varied to investigate the effect of top-bottom capacitances. Fig. 5(c) shows the simulated reflection coefficients obtained from the equivalent circuit model and the full-wave EM simulations. Geometric parameters used in the circuit models and full-wave simulations are listed in Table 2. As the width of the rectangular defect increases, the capacitances between the top and bottom conductors decrease and alter the transmission band.

Table 2. Geometric and electrical parameters of the rectangular DGS shown in Fig. 5. (Unit of X and Y: mm).

Item	X	Y	C_1 (pF)	C_s (pF)	L_1 (nH)	L_p (nH)
case1	4	16	0.211	0.2	2.55	0.91
case2	5	16	0.203	0.2	2.55	1.701
case3	7	16	0.197	0.2	2.55	2.965

2.2.1. A Single Finger-Shape DGS Microstrip

Figure 6(a) shows a 3D schematic diagram of the finger-shape DGS microstrip line. For this configuration, the capacitances between the top metallic strips and bottom ground were different at the finger regions and hollow areas. The top-bottom capacitances at the region of the finger was strong than that at the hollow region and affected the series inductances of the microstrip lines. Therefore, the finger-shape DGS was divided into two regions shown in Fig. 6(b) where C_1 was the top-bottom capacitance at the hollow region, C_2 represented the top-bottom capacitances at the region of the finger, L_1 indicated the series inductance at the hollow region, and L_1 indicated the series inductance at the region of the finger. The finger-shape DGS had the circumference resonance acting as a parallel LC resonator. The equivalent circuit model is presented in Fig. 6(c). Fig. 6(d) shows the simulated transmission and reflection coefficients obtained from the circuit model and full-wave EM simulations. The lowpass response was due to the lowpass LC resonators composed of C_1, C_2, L_1, and L_2. The transmission notch at 2.32 GHz corresponded to the parallel LC resonator composed of C_p and L_p. The transmission pole of 8.5 GHz was based on series resonator composed of the capacitor, C_p, and the series inductors, L_2. The electrical parameters exploited in the simulations are listed in Table 3.

Table 3. The electrical parameters utilized in the simulations shown in Fig. 6.

C_1	0.37 (pF)	C_2	0.88 (pF)	C_p	3.025 (pF)
L_1	0.28 (nH)	L_2	0.3 (nH)	L_p	1.51 (nH)

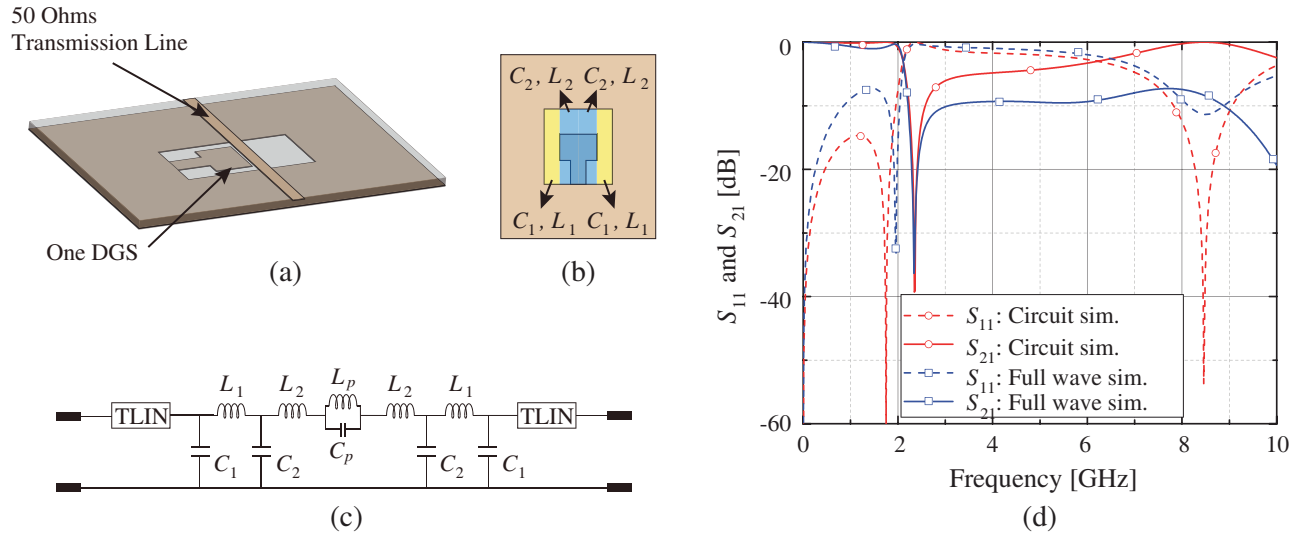

Figure 6. (a) The 3D schematic diagram of a finger-shape-DGS lowpass filter. (b) The bottom view. The DGS was divided into two regions to discuss the differences of the capacitances between the top and bottom electrodes at the finger and the hollow regions. (c) The equivalent circuit model where the parallel LC resonator represented the resonance of the finger-shape DGS. (d) The simulated transmission and reflection coefficients. The transmission pole was due to the series LC resonator composed of L_2 and C_p.

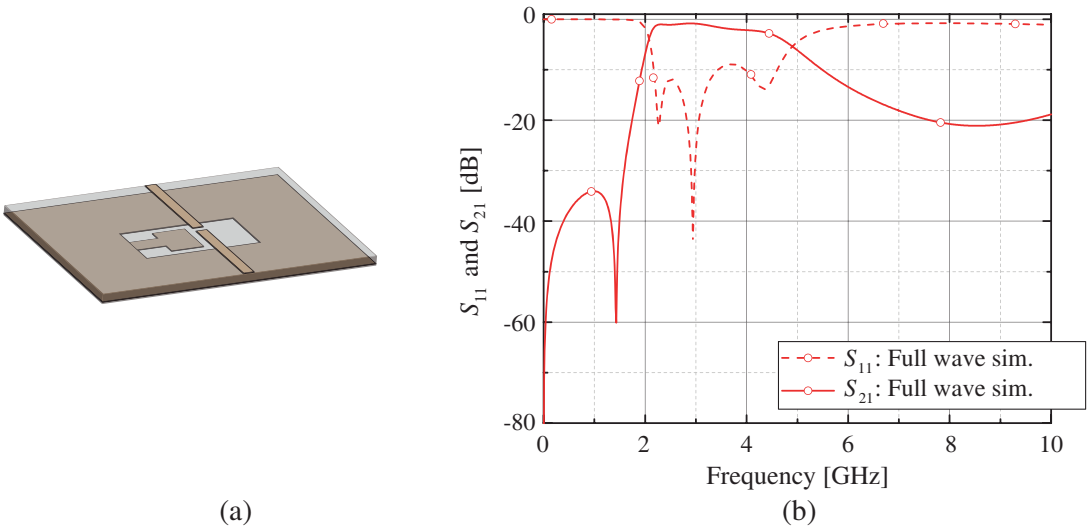

Figure 7. (a) The 3D topology of a finger-shape DGS bandpass filter composed of a finger-shape DGS and a capacitive microstrip gap. (b) Simulated transmission and reflection coefficients obtained from the full-wave EM simulations. The three transmission poles were due to the series LC resonators composed of the capacitance, C_s, and inductors, L_1 and L_2. The transmission notch was caused by the parallel resonator due to the self-resonance of the DGS.

2.2.2. Combined with Microstrip Gaps

Although a single finger-shape DGS demonstrated a lowpass response due to the series inductors, a capacitive microstrip gap described in Fig. 5 could be exploited to convert lowpass responses to a bandpass responses. Fig. 7(a) shows the 3D topology of the finger-shape DGS combined with a capacitive microstrip gap. The simulated frequency responses obtained from the full-wave EM simulations are

shown in Fig. 7(b). This filter demonstrated a third-order bandpass response based on the series LC resonators composed of the capacitance, C_s, and inductors, L_1 and L_2. The transmission notch at 1.45 GHz depended on the parallel LC resonator due to the self resonance of the finger-shape DGS.

2.3. Final Design of Combining SIR and Finger-Shape DGSs

In order to achieve the design goal of a steep roll-off response and wide out-of-band rejections, two finger-shape DGSs were exploited to increase the order of the filter and a SIR was utilized to shift the spurious frequencies out of the interested frequency range. The final design is shown in Fig. 1(a) and the geometric dimensions were listed in Table 1. Fig. 8 shows the simulated transmission and reflection coefficients obtained from the full-wave EM simulations. The finger-shaper DGS filter demonstrated a high-order bandpass response covering the ISM band and a wide out-of-band rejections up to 20 GHz. As mentioned in the previous section, each finger-shape DGS contributed three transmission poles in the passband. The transmission zeros at 0.6 GHz and 1.2 GHz were due to the self resonances of finger-shape DGS. In addition, the SIR contributed one transmission pole and one transmission notch at 4.5 GHz. Therefore, the finger-shape DGS bandpass filter had a wide bandwidth and a sharp roll-off response.

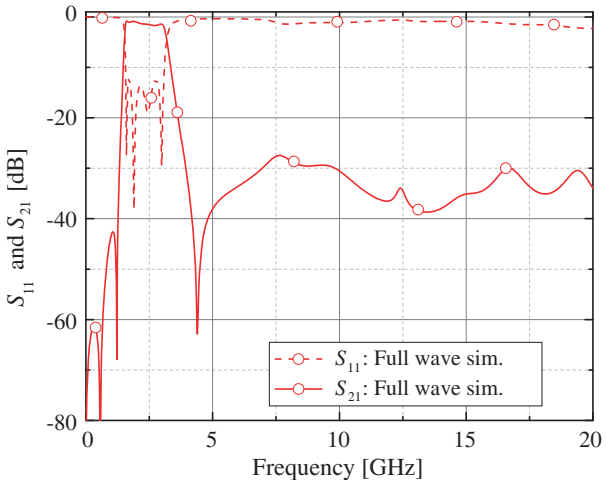

Figure 8. The simulated frequency responses of the finalized finger-shape DGS microstrip filter obtained from the full-wave simulations.

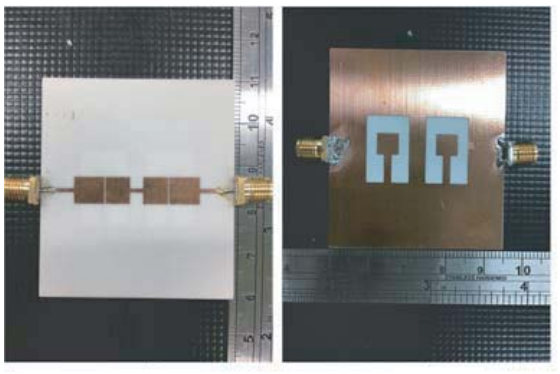

Figure 9. Photographs of the fabricated finger-shape DGS bandpass filter. (a) Top view. (b) Bottom view.

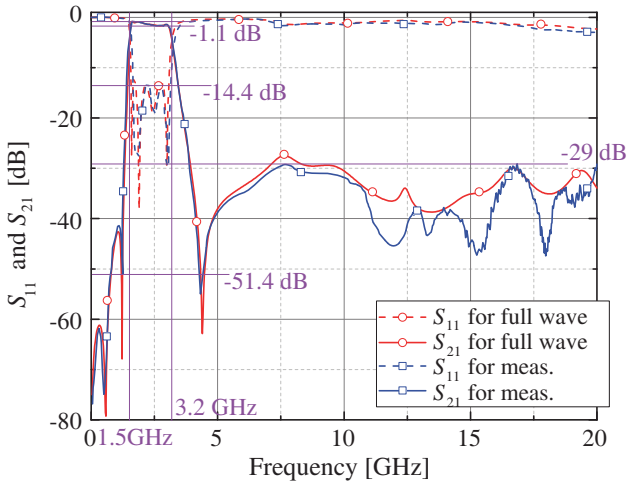

Figure 10. The transmission and reflection coefficients obtained from the full-wave EM simulations and measurements.

3. FABRICATIONS AND MEASUREMENTS

A prototype was fabricated with the standard PCB lithography. For high frequency applications, we used Rogers RO4003C as the dielectric substrate with the dielectric constant of $\epsilon = 3.55$, loss tangent of 0.0027, and the thickness of $h = 0.508$ mm. Fig. 9 shows the photographs of the fabricated filter. Its frequency response was measured with a calibrated vector network analyzer (Agilent E5071C) shown in Fig. 10. The fabricated finger-shape filter demonstrated a passband centered at 2.35 GHz with the fractional bandwidth of 72.3%, insertion loss below 1.1 dB, and a stop-band rejections of −29 dB up to 20 GHz. The simulated result matched with the measured results.

4. DISCUSSIONS

4.1. Comparisons with Other Work

Spurious-suppressed band-pass filters have been investigated by lots of research groups where SIR and DGS are the two commonly-used approaches. In this section, we compare our finger-shape DGS bandpass filter with other published harmonic-suppressed work shown in Table 4. The main differences are the bandwidth and the order of the bandpass filter. Most harmonic-suppressed filters have narrow bandwidths smaller than 10% but the bandwidth of our device is more than 70% due to the high order and large inductances of finger-shape DGSs. Since DGSs can increase the ground current paths, the series inductances are enhanced and the bandwidth of each LC resonator increase as well. In addition, high-order finger-shape DGS bandpass filter provides a sharp roll-off response and large out-of-band rejections up to $8.5 \times f_0$.

Table 4. Comparisons with some published harmonic-suppressed BPFs.

Ref.	f_0	N	FBW	IL (dB)	RL (dB)	R. (dB)	S. f_0	Size (λ_0^2)	FOM	Method
[7]	1.5	5	10 %	3	20	−30	$6.5f_0$	0.029	12,622	SIR
[8]	2.04	4	7.6%	2.6	−21	25	$11.4f_0$	0.026	15,323	SIR
[15]	2	3	10%	2.45	18.8	−30	$4f_0$	0.049	10,766	DGS
[16]	2.48	4	10.8%	1.08	23.8	−30	$12.1f_0$	0.058	15,455	DGS
[17]	2.44	-	3.3%	1.93	20	−25	6.55 f_0	0.017	19,059	DGS
[18]	2.3	-	4.5%	0.67	22	−20	4.35 f_0	0.082	2,843	Shorted Symmetrical
[19]	1.15	4	33%	1.1	16	−40	7 f_0	0.014	12,526	Multi-Layer
[20]	6	3	9 %	1	-	−32	$2.2f_0$	-	-	Grooves in PCML
[21]	5	3	35 %	-	20	−30	$1.8f_0$	-	-	DGS
This work	2.35	7	72.3%	< 1.1	14.4	−29	$8.5f_0$	0.034	3,970	DGS + SIR

N: order of filter FBW: fractional bandwidth IL: insertion loss RL: return loss FOM: figure of merit [22]

One characteristic of the finger-shape DGS bandpass filter is the compact size of $0.23\lambda_0 \times 0.15\lambda_0$. If other harmonic-suppressed filters increase the order of the filter by adding more SIRs or DGSs, this might increase the occupied areas and enlarge the overall dimensions.

5. CONCLUSIONS

In this research, we proposed a compact, high-order, and harmonic suppressed bandpass microstrip filter by combining three filter design techniques including stepped impedance resonator (SIR), defected ground structure (DGS), and series capacitively coupling resonator. In contrast to a conventional DGS acting as a single parallel resonator, we presented a finger-shape DGS which could created multiple resonators leading to a high-order frequency response. By exploiting two finger-shape DGSs and a SIR, our bandpass filter demonstrated a seventh-order bandpass response with a steep skirt selectivity, wide out-of-band rejections up to 20 GHz, and a compact size.

ACKNOWLEDGMENT

The authors would like to thank Prof. Chao-Hsiung Tseng (National Taiwan University of Science and Technology) for giving accesses to his facilities and helpful suggestions. This work was supported by Ministry of Science and Technology, Taiwan, under funding No. 106-2221-E-002-219-MY2.

REFERENCES

1. Barth, C., I. R. Linscott, and U. S. Inan, "An image frequency rejection filter for SAW-less GPS receivers," *IEEE Transactions on Circuits and Systems I: Regular Papers*, Vol. 59, No. 5, 1085–1092, 2012.
2. Chaudhary, G., Y. Jeong, and J. Lim, "Harmonic suppressed dual-band bandpass filters with tunable passbands," *IEEE Transactions on Microwave Theory and Techniques*, Vol. 60, No. 7, 2115–2123, 2012.
3. Zhang, X. Y., Q. Xue, C. H. Chan, and B. J. Hu, "Low-loss frequency-agile bandpass filters with controllable bandwidth and suppressed second harmonic," *IEEE Transactions on Microwave Theory and Techniques*, Vol. 58, No. 6, 1557–1564, 2010.
4. Tu, W.-H. and K. Chang, "Compact second harmonic-suppressed bandstop and bandpass filters using open stubs," *IEEE Transactions on Microwave Theory and Techniques*, Vol. 54, No. 6, 2497–2502, 2006.
5. Chaudhary, G., Y. Jeong, and J. Lim, "Dual-band bandpass filter with independently tunable center frequencies and bandwidths," *IEEE Transactions on Microwave Theory and Techniques*, Vol. 61, No. 1, 107–116, 2013.
6. Huynh, C. and C. Nguyen, "New technique for synthesizing concurrent dual-band impedance-matching filtering networks and 0.18 µm SiGe BiCMOS 25.5/37-GHz concurrent dual-band power amplifier," *IEEE Transactions on Microwave Theory and Techniques*, Vol. 61, No. 11, 3927–3939, 2013.
7. Kuo, J. T. and E. Shih, "Microstrip stepped impedance resonator bandpass filter with an extended optimal rejection bandwidth," *IEEE Transactions on Microwave Theory and Techniques*, Vol. 51, No. 5, 1554–1559, 2003.
8. Lin, S.-C., P.-H. Deng, Y.-S. Lin, C.-H. Wang, and C. H. Chen, "Wide-stopband microstrip bandpass filters using dissimilar quarter-wavelength stepped-impedance resonators," *IEEE Transactions on Microwave Theory and Techniques*, Vol. 54, No. 3, 1011–1018, 2006.
9. Kuo, J.-T., T.-H. Yeh, and C.-C. Yeh, "Design of microstrip bandpass filters with a dual-passband response," *IEEE Transactions on Microwave Theory and Techniques*, Vol. 53, No. 4, 1331–1337, 2005.
10. Aziz, M. A., A. M. E. Safwat, F. Podevin, and A. Vilcot, "Coplanar waveguide filters based on multibehavior etched-ground stubs," *IEEE Transactions on Components and Packaging Technologies*, Vol. 32, No. 4, 816–824, 2009.
11. Barakat, A., R. Pokharel, and T. Kaho, "60 GHz on-chip mixed coupled BPF with H-shaped defected ground structures," *Electronics Letters*, Vol. 52, No. 7, 533–535, 2016.
12. Chen, H. J., T. H. Huang, C. S. Chang, L. S. Chen, J. H. Horng, Y. H. Wang, and M. P. Houng, "A compact bandpass filter with enhanced stopband characteristics by an asymmetric cross-shape defected ground structure," *IEEE Transactions on Ultrasonics, Ferroelectrics, and Frequency Control*, Vol. 53, No. 11, 2183–2187, 2006.
13. Abdel-Rahman, A., A. K. Verma, A. Boutejdar, and A. S. Omar, "Compact stub type microstrip bandpass filter using defected ground plane," *IEEE Microwave and Wireless Components Letters*, Vol. 14, No. 4, 136–138, 2004.
14. Park, J.-S., J.-S. Yun, and D. Ahn, "A design of the novel coupled-line bandpass filter using defected ground structure with wide stopband performance," *IEEE Transactions on Microwave Theory and Techniques*, Vol. 50, No. 9, 2037–2043, 2002.

15. Karshenas, F., A. R. Mallahzadeh, and J. Rashed-Mohassel, "Size reduction and harmonic suppression of parallel coupled-line bandpass filters using defected ground structure," *2009 13th International Symposium on Antenna Technology and Applied Electromagnetics and the Canadian Radio Science Meeting*, 1–6, 2009.
16. Luo, X., J. G. Ma, E. P. Li, and K. Ma, "Hybrid microstrip T-stub/defected ground structure cell for electromagnetic interference bandpass filter design," *IEEE Transactions on Electromagnetic Compatibility*, Vol. 53, No. 3, 717–725, 2011.
17. Luo, X. and J. G. Ma, "Compact slot-line bandpass filter using backside microstrip open-stubs and air- bridge structure for spurious suppression," *2009 Asia Pacific Microwave Conference*, 882–885, 2009.
18. Luo, X., H. Qian, J. G. Ma, and K. S. Yeo, "A compact wide stopband microstrip bandpass filter using quarter-wavelength shorted coupled-lines," *2010 Asia-Pacific Microwave Conference*, 1142–1145, 2010.
19. Chen, J. X., Y. L. Li, W. Qin, Y. J. Yang, and Z. H. Bao, "Compact multi-layer bandpass filter with wide stopband using selective feeding scheme," *IEEE Transactions on Circuits and Systems II: Express Briefs*, Vol. 65, No. 8, 1009–1013, 2017.
20. Kumar, A. and G. Bharti, "Spurious response suppression using triple grooves in PCML bandpass filter," *2017 International Conference on Innovations in Information, Embedded and Communication Systems (ICIIECS)*, 1–3, 2017.
21. Pal, B. and S. Dwari, "A compact parallel coupled wideband bandpass filter with DGS and spurline," *2015 International Conference on Microwave and Photonics (ICMAP)*, 1–2, 2015.
22. Hayati, M., H. A. Memari, and H. Abbasi, "Compact microstrip lowpass filter with sharp roll-off and wide stopband using semicircle ended stub resonator," *Progress In Electromagnetics Research Letters*, Vol. 35, 73–81, 2012.